Physical Biology

NOTE

Single file diffusion into a semi-infinite tube

Spencer G Farrell, Aidan I Brown and Andrew D Rutenberg

Department of Physics and Atmospheric Science, Dalhousie University, Halifax, NS, B3H 4R2, Canada

E-mail: andrew.rutenberg@dal.ca

Keywords: single-file diffusion, microtubules, alpha-TAT1, k-order statistics

RECEIVED
9 June 2015

REVISED
26 September 2015

ACCEPTED FOR PUBLICATION
2 October 2015

PUBLISHED
20 November 2015

Abstract

We investigate single file diffusion (SFD) of large particles entering a semi-infinite tube, such as luminal diffusion of proteins into microtubules or flagella. While single-file effects have no impact on the evolution of particle density, we report significant single-file effects for individually tracked tracer particle motion. Both exact and approximate ordering statistics of particles entering semi-infinite tubes agree well with our stochastic simulations. Considering initially empty semi-infinite tubes, with particles entering at one end starting from an initial time $t = 0$, tracked particles are initially super-diffusive after entering the system, but asymptotically diffusive at later times. For finite time intervals, the ratio of the net displacement of individual single-file particles to the average displacement of untracked particles is reduced at early times and enhanced at later times. When each particle is numbered, from the first to enter ($n = 1$) to the most recent ($n = N$), we find good scaling collapse of this distance ratio for all n. Experimental techniques that track individual particles, or local groups of particles, such as photo-activation or photobleaching of fluorescently tagged proteins, should be able to observe these single-file effects. However, biological phenomena that depend on local concentration, such as flagellar extension or luminal enzymatic activity, should not exhibit single-file effects.

Introduction

Single-file diffusion (SFD) describes a one-dimensional system of diffusing particles that cannot pass one another—essentially diffusion with collisions [1]. Hard-core repulsive interactions keep particles in the same order, without affecting their collective motion. This is in contrast to simple diffusive processes without interactions, where particles can exchange their order as they pass each other.

SFD can be realized experimentally with hard-core particles in a relatively narrow channel, and can be easily visualized in colloidal systems [2]. SFD can exhibit subdiffusive, mean-square displacement (MSD) $\sim t^{1/2}$, behaviour [3–9]. This subdiffusive behaviour of tracer particles is due to the no-crossing constraints imposed by adjacent particles, and differs from the standard MSD $\sim t$ behaviour of simple-diffusion (SD) [10]. The actual behaviour for SFD depends on both the initial conditions and the boundary conditions of the system [3, 7, 11, 12]. Notably, starting particles in a tight cluster leads to initially ballistic motion [12], while a tracer particle at the edge of a Gaussian cluster of particles asymptotically exhibits MSD $\sim t$ at late times but with a single-particle diffusivity D that is enhanced by the logarithm of the number of particles N in the cluster, so that $\langle x_N \rangle \simeq \sqrt{\ln N}\sqrt{4Dt}$ [11]. Subdiffusive MSD$\sim t^{1/2}$ for tracer-particle displacement applies only to SFD with a uniform-density.

While tracer particle behaviour in single-file systems is generally not diffusive, the evolving density profile in a single-file system *is* simply diffusive and is the same between SD and SFD [1, 10, 13]. This is because single-file effects can be implemented in unbiased diffusive systems by simply exchanging particle identities when particles change order. This exchange of particle identities leaves densities unchanged [1]. While biased random walks can have distinct collective behaviour with SFD [14], we only consider unbiased diffusion in this paper. We are interested in tracer particle dynamics, since they can be easily characterized with fluorescently labelled proteins.

Luminal αTAT1 catalyzes the post-translational acetylation of microtubules [15, 16]. αTAT1 appears to enter the microtubule from one end [17], and subsequently diffuses [18]. Motivated by this, we consider SFD of particles into one end of an initially empty semi-infinite one-dimensional channel. While single-

file effects in finite channels have been previously considered, it was only with initially full tubes that subsequently empty [19]. A classic study by Odde [20] considered diffusion into microtubules, but did not consider single-file effects. Microtubules have an inner radius of 7 nm [16] and αTAT1 has a radius of 3.5 nm [16], or half the microtubule inner radius, suggesting SFD may occur for αTAT1 inside microtubules.

In this paper, we consider the behaviour of luminal particles entering into, and diffusing inside, microtubules. We model the microtubules as a homogeneous 1D tube, initially empty, where particles enter at one end (tip) and diffuse along the length. Our model system is semi-infinite, since we are studying the transient regime where the particles are entering the tube.

Methods and analysis

More precisely, we consider the average occupation density $\rho(x, t)$ for a semi-infinite interval $x \in [0, \infty)$ that is initially empty, with $\rho(x, t = 0) = 0$. We are interested in the dynamics of invasion from a bulk reservoir that imposes a constant density at the tip, $\rho(x = 0, t) = \rho_{\text{tip}}$. For example, this would correspond to an *in vitro* experiment in which a fixed concentration of αTAT1 was imposed around a collection of initially empty microtubules. The average density is given by the solution of the diffusion equation, so that $\rho(x, t) = \rho_{\text{tip}}\,\text{erfc}(x/\sqrt{4Dt})$, where D is the single-particle diffusivity and erfc is the complimentary error function [20, 21]. Integrating this we expect that the average number of luminal particles near each tube-tip increases with

$$N(t) = \rho_{\text{tip}}\sqrt{4Dt/\pi}\,. \tag{1}$$

What do we expect for tracer particles with single-file diffusion? The normalized probability density is

$$\hat{\rho}(x, t) \equiv \text{erfc}\left(x/\sqrt{4Dt}\right)\sqrt{\pi/(4Dt)}\,, \tag{2}$$

where $\int_0^\infty \hat{\rho}\,\mathrm{d}x = 1$. With N single-file particles, there is a distinct probability distribution for the position of each particle, i.e. each of the random variables $x_1, x_2, \ldots, x_N$ where x_1 is first to enter (i.e. furthest from the tip) while x_N is last to enter (i.e. closest). Using k-order statistics [11, 22] the probability distribution for the position of the nth particle , which is farther from the the tube tip than $N-n$ particles, and closer to the tube entrance than $n-1$ particles, is

$$q_n\left(x_n, t\right) = \frac{(N-1)!}{(N-n)!\,(n-1)!}\left[\int_0^{x_n}\hat{\rho}(x, t)\,\mathrm{d}x\right]^{N-n} \times \hat{\rho}\left(x_n, t\right)\left[\int_{x_n}^{\infty}\hat{\rho}(x, t)\,\mathrm{d}x\right]^{n-1}. \tag{3}$$

Equation (3) originates from a binomial distribution and is a product of four terms. The first, combinatorial, term accounts for the order combinations of the particles. The second term, with exponent $N-n$, is the probability that $N-n$ particles are closer to the tube tip than the nth particle. The third term is the probability density of a single (the nth) particle. The fourth term, with exponent $n-1$, is similar to the second term and is the probability that $n-1$ particles are further from the tube tip than the nth particle. Equation (3) can be maximized with respect to x_n to find the most likely x_n^*. In the limits of n, N, and $N-n \gg 1$, we obtain an implicit equation,

$$\int_0^{x_n^*}\hat{\rho}\,\mathrm{d}x \simeq 1 - \frac{n}{N}, \tag{4}$$

which is identical to the analogous expression of Gumbel [22].

Equation (4) implies that each particle occupies a $1/N$ fraction of the integrated probability density, so that the first n particles to enter the tube will occupy n/N of the integrated probability density. However, the average position of the nth particle should correspond to halfway through its share of the integrated probability density, so that $\int_0^{\langle x_n\rangle}\hat{\rho}\,\mathrm{d}x = 1 - (n-1/2)/N$. This should apply to all n and N. In the approximation that the most likely position x_n^* equals its average position, which holds when the k-order statistics are sharply peaked [11], we then obtain

$$\int_0^{x_n^*}\hat{\rho}\,\mathrm{d}x \simeq 1 - \frac{n-1/2}{N}. \tag{5}$$

This equation asymptotically equals equation (4) when n, $N \gg 1$. The integral on the left-hand-side can be evaluated exactly, yielding an implicit equation for x_n^* that we solve numerically,

$$\exp\left(-x_n^{*2}/(4Dt)\right) - \frac{x_n^*}{\sqrt{4Dt}} \times \sqrt{\pi}\,\text{erfc}\left(x_n^*/\sqrt{4Dt}\right) = \frac{n-1/2}{N}. \tag{6}$$

Below, we find with stochastic simulations that equations (5) and (6) are accurate even for small n and N.

We use stochastic simulations to investigate the dynamics of the single file system, to compare with our analytical results. We discretize our tube with a uniform lattice spacing Δx. After each timestep Δt, $N(t)$ particles are chosen randomly with replacement to each attempt to move randomly to the right or left with equal probability. To enforce the SFD condition, moves that lead to multiple occupancy are prohibited.

The occupation probability at the entrance is completely enforced by the quantity p_{tip}. At the end of each timestep, the occupancy of the entrance lattice site at $x = 0$ is set to one with probability p_{tip}, and to zero with probability $1 - p_{\text{tip}}$. This p_{tip} occupancy condition at the entrance is the mechanism by which additional particles are introduced to the tube. Since we track the nth particle after its first appearance at time t_n, control of the occupancy of the entrance site by p_{tip}

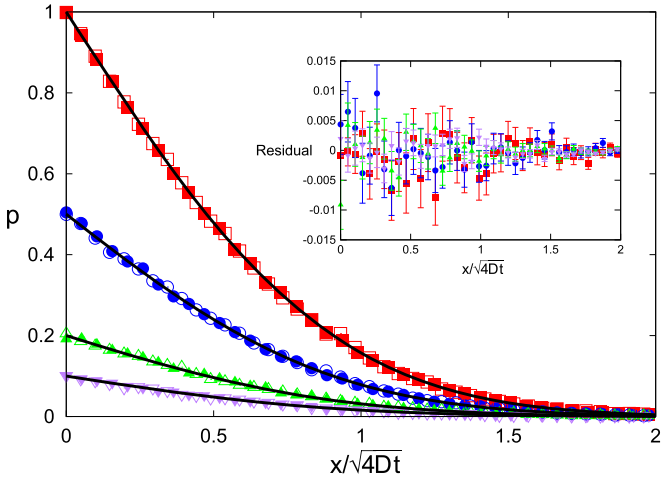

Figure 1. Average particle density $p(\tilde{x})$ versus scaled distance $\tilde{x} \equiv x/\sqrt{4Dt}$ along the semi-infinite 1D system. Points show the mean occupation fraction for discrete stochastic SFD simulations at two distinct times (unfilled points at $t = 4.6 \times 10^6$ and filled at $t = 4.6 \times 10^7$), with fixed tip occupation probabilities $p_{\text{tip}} = 1, 0.5, 0.2$ and 0.1 (red squares, blue circles, green upward pointing and purple downward pointing triangles, respectively). Thin black lines indicate analytic diffusion results, from equation (2), scaled to p_{tip} at $\tilde{x} = 0$. The inset shows the residuals, or differences between simulation and analytical results, at $t = 4.6 \times 10^7$, with statistical error bars.

means that reflecting and absorbing boundary conditions on particle motion at the tip are fully equivalent. We vary $p_{\text{tip}} \in (0, 1]$.

For simplicity, we use units in which $\Delta x = \Delta t = 1$, corresponding to $D = \Delta x^2/(2\Delta t) = 0.5$. When shown, error bars are statistical error bars over 1000 independent stochastic simulations.

Results

First, we consider the occupation probability within the semi-infinite tube. In figure 1, we plot the average occupation probabilities of our stochastic single-file simulation for two distinct times and various values of p_{tip} (shown with points). At both times, the agreement with equation (2), scaled to the imposed p_{tip} and shown with solid lines, is striking. As shown by the residuals in the inset, any systematic effects due to the imposition of single-occupancy in our simulation are currently too small to resolve, which confirms that SFD has essentially the same collective behaviour as simple diffusion [7, 9, 19]. The absence of SFD effects in particle density implies that dynamical processes, such as microtubule acetylation [15–18], that do not distinguish between diffusing particles, should behave identically with or without single-file effects.

While the dynamics of the average density are not changed by SFD, the behaviour of individually tracked SFD particles is significantly different than in SD. Figure 2 shows the average position of the nth tracked particle from the tip versus time. Our stochastic simulation results are shown with points, where averages are over particles that are still in the tube at time t. Numerical solutions of x_n^* from equation (6) are shown with solid lines, where we use N from equation (1). We see that equation (6) is a good approximation for all t.

To evaluate the diffusive, subdiffusive, or super-diffusive nature of the tracked particle motion, we plot $\langle x_n \rangle$ against the time since the nth particle entered the tube, i.e. $t - t_n$ where t_n is the time the particle entered the tube. The inset of figure 2 shows that $\langle x_n \rangle$ initially grows superdiffusively, with position increasing faster than $(t - t_n)^{1/2}$, and asymptotically approaches diffusive behaviour, where position increases as $(t - t_n)^{1/2}$. Such early super-diffusion of tracked SFD particles occurs when there is a density gradient [12]. In our case, this gradient is from the tip (as shown in figure 1) but decreases in magnitude as time increases since the characteristic length-scale of the diffusive density field grows with time.

We also evaluate a squared distance ratio, $R_n = \langle x_n \rangle^2 / \langle x \rangle^2$, the ratio between the squared average position of the nth tracer particle, $\langle x_n \rangle^2$, and the average bulk position squared, $\langle x \rangle^2$, where $\langle x \rangle = \sqrt{\pi Dt/4}$ is found by averaging over equation (2). The squared distance ratio R_n can provide information on how tracer particle motion differs from particle motion in the bulk, despite equal average densities in the tube. In figure 3 we plot R_n vs. $N(t)/(n - 1/2)$. The scaling with $N/(n - 1/2)$ is predicted by the right-side of equation (6). We observe good scaling collapse for different n and different p_{tip}, indicating that the essential physics of single-file effects are similar for different n and different overall densities.

The average bulk particle position $\langle x \rangle$ does not depend on the presence of single-file effects, as demonstrated in figure 1. Therefore, we see in figure 3 that single file particles that have recently entered the tube (N not significantly larger than n) are closer to the tube entrance than the average bulk position of all particles,

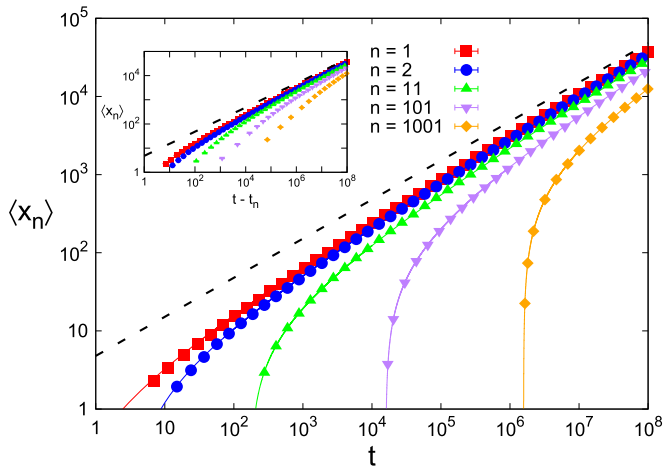

Figure 2. Average particle position $\langle x_n \rangle$ versus time, using $p_{\text{tip}} = 1$. The results from stochastic simulations are shown as coloured points, as indicated, while the numerical solutions of equation (6) are shown as correspondingly coloured solid lines. The black dashed line illustrates $x_n \sim t^{1/2}$, i.e. diffusive motion. The inset shows $\langle x_n \rangle$ versus the time the nth particle has been in the tube, $t - t_n$, as well as a black dashed line for $\langle x_n \rangle \sim (t - t_n)^{1/2}$. Statistical error bars for numerical data are smaller than the data points.

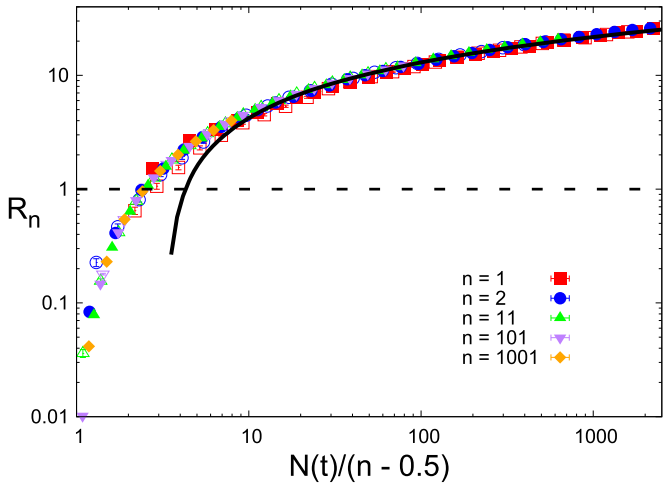

Figure 3. Squared distance ratio $R_n \equiv \langle x_n \rangle^2 / \langle x \rangle^2$ versus scaled particle number $N(t)/(n - 1/2)$, for various tracked particle number n as indicated. $\langle x_n \rangle$ is the average position of the nth tracked particle, $\langle x \rangle = \sqrt{\pi D t/4}$ is the average particle position from equation (2), and $N(t)$ is the total number of particles in the tube. The dashed horizontal line shows $R_n = 1$, where the $\langle x_n \rangle = \langle x \rangle$. Points are from stochastic simulation, using both $p_{\text{tip}} = 1$ (filled points) and $p_{\text{tip}} = 0.1$ (unfilled points). Statistical error bars are shown. The solid black line illustrates the expected $\log(N/(n - 1/2))$ asymptotic behaviour at large N from equation (6).

i.e. $R_n < 1$, as expected. After more particles have entered the tube, with $N/(n - 1/2) \simeq 2.5$, the average position of the nth particle is equal to the average position of all particles, i.e. $R_n = 1$. In figure 2, particles which have recently entered the tube behave super-diffusively and trend towards diffusive behaviour at later times. Figure 3 shows a similar effect, as R_n versus $N/(n - 0.5)$ initially has a relatively large slope, and flattens out as N increases. For large N, as illustrated by the solid black line in figure 3, we observe $R_n \sim \log(N/(n - 1/2))$. This dependence can be extracted from equation (6) by Taylor expansion of the erfc, and solving for the leading behaviour of $x_n^2 \sim t \log(N/(n - 1/2))$. This gives $R_n \simeq x_n^2/\langle x \rangle^2 \sim \log(N/(n - 1/2))$. This $R_n \sim \log N$ dependence is essentially the same as the $\log N$ drift enhancement reported by Aslangul for the leading particle within an expanding cluster [11].

Discussion

We have described particles entering into and then diffusing single-file within tubes. Consistent with previous studies [7, 9, 19], the evolution of the average density with unbiased SFD is identical to simple diffusion (SD) [1, 10, 13], as shown in figure 1. This is because SFD can be recovered from SD by swapping particle labels upon collisions [1], and this has no effect on density dynamics.

We emphasize that anomalous tracer diffusion with SFD does not imply either enhanced or hindered

bulk transport. Stern and Berg [23] model the growth of bacterial flagellar filaments by SFD of flagellin subunits through the flagellar lumen and addition at the distal flagellar tip. However, because the diffusive transport determines the flagellar growth, either SD or SFD should give identical results. Similarly, Yang *et al* [24] contrast single-file (constant rate) and 'Fickian' (time-dependent rate) release profiles of drugs through cylindrical nanochannels, while SFD should provide the same density dynamics as SD.

We observe single-file effects in traced individual particles. Figure 2 shows that individual single-file particles have super-diffusive behaviour immediately after entering the tube, and then slowly trend towards $\langle x^2 \rangle \sim t$ diffusive behaviour. We also find that individual particles experience a steady increase in the ratio of average tracer position to average bulk position, with figure 3 demonstrating that this exhibits scaling collapse across all traced particles in the system.

SFD requires that diffusing particles are of comparable size with the tube dimensions. Two additional physical effects are correlated with these large particle sizes. The first is significantly slower single-particle transport (D) due to wall-mediated drag [20]. The second is an upper limit imposed on the local luminal density achieved by close-packing of particles. We have included this latter effect in our stochastic lattice-based SFD model, with a single-occupancy condition. As seen in figure 2 the single-occupancy condition alone, at the highest local densities, does not lead to significant differences in transport compared to SD. When SFD is observed, this implies that reduced single-particle diffusivity due to wall-mediated drag is the primary physical effect expected for enzymatic activity, such as microtubule acetylation by luminal αTAT1 enzymes [17].

Biologically relevant values of p_{tip} for αTAT1 may be estimated with diffusion-limited rates [25]. With free diffusivity $\mathrm{D} = 79.3\,\mu\mathrm{m}^2\,\mathrm{s}^{-1}$ [18], MT radius $s = 7\,\mathrm{nm}$ [16], and concentration $\rho = 0.17\,\mu\mathrm{M}$ [26, 27], the diffusion-limited [25] influx rate can be estimated at $\Gamma = 4sD\rho = 220$ molecules per second. With the inner MT diffusivity $0.27\mu\mathrm{m}^2\,\mathrm{s}^{-1}$ [18], a typical distance traveled by a freely diffusing particle in 1d in the time before another molecule enters is 50 nm, suggesting one molecule would typically move approximately seven lengths before another arrives, giving $p_{\text{tip}} \approx 0.14$. Other factors could increase this estimate of p_{tip}, such as elevated αTAT1 concentration at clathrin coated pit sites proposed for αTAT1 influx [17], or for *in vitro* experiments [16, 18], or the presence of single file particles blocking the progress of a recently entered particle. Indeed, cryoelectron microscopy of MT from neuronal processes in brain tissue shows closely spaced luminal particles with approximately 3.5 nm radius [28]. This suggests crowding effects may be significant in at least some MT, including SFD effects of tracked particles.

While transport is determined by the single-particle diffusivity D, measuring D through the motion of individual fluorescently labeled particles over longer timescales must take into account any single-file effects. One approach is to limit tracking to short timescales to avoid particle collisions [18]. However, for longer timescales inferring D and/or inferring SFD is straight-forward: particle position in time depends on the sequence that particles enter the tube—in our model, this dependence is on the value of n (through equation (6) and figures 2 and 3). We note that FRAP (fluorescence recovery after photobleaching) [29] will be qualitatively different with SFD—since there can be no invasion of fluorescent particles into bleached regions. We would expect local bleached plugs of particles to slowly move and expand as the left and right ends move apart, with average position $(x^*_{\text{left}} + x^*_{\text{right}})/2$ and width $(x^*_{\text{left}} - x^*_{\text{right}})$, with similar results for locally photoactivated regions. In light of SFD effects on tracked fluorescent particles, assessing single-particle diffusivity D by fitting density profiles using equation (2) is probably the simplest approach.

Acknowledgments

ADR thanks the Natural Science and Engineering Research Council (NSERC) for operating grant support (RGPIN-2014-06245). SGF thanks NSERC for summer USRA fellowship support, and AIB thanks NSERC, the Sumner Foundation, and the Killam Trusts for fellowship support. We all thank the Atlantic Computational Excellence Network (ACEnet) for computational resources. We thank Guillaume Montagnac for introducing us to the αTAT1 system.

References

[1] Harris T E 1965 Diffusion with 'collisions' between particles *J. Appl. Prob.* **2** 323–38
[2] Wei Q-H, Bechinger C and Leiderer P 2000 Single-file diffusion of colloids in one-dimensional channels *Science* **287** 625–7
[3] Lizana L and Ambjörnsson T 2008 Single-file diffusion in a box *Phys. Rev. Lett.* **100** 200601
[4] Suarez G, Hoyuelos M and Mártin H O 2013 Evolution equation for tagged-particle density and correlations in single file diffusion *Phys. Rev.* E **88** 022131
[5] Taloni A and Lomholt M A 2008 Langevin formulation for single-file diffusion *Phys. Rev.* E **78** 051116
[6] Ambjörnsson T, Lizana L, Lomholt M A and Silbey R J 2008 Single-file dynamics with different diffusion constants *J. Chem. Phys.* **129** 185106
[7] Lizana L, Lomholt M A and Ambjörnsson T 2014 Single-file diffusion with non-thermal initial conditions *Physica* A **395** 148–53
[8] Lizana L and Ambjörnsson T 2009 Diffusion of finite-sized hard-core interacting particles in a one-dimensional box: tagged particle dynamics *Phys. Rev.* E **80** 051103
[9] Lomholt M A, Lizana L and Ambjörnsson T 2011 Dissimilar bouncy walkers *J. Chem. Phys.* **134** 045101
[10] van Beijeren H, Kehr K W and Kutner R 1983 Diffusion in concentrated lattice gases: III. Tracer diffusion on a one-dimensional lattice *Phys. Rev.* B **28** 5711–23

[11] Aslangul C 1998 Classical diffusion of N interacting particles in one dimension:general results and asymptotic laws *Europhys Lett.* **44** 284–9
[12] Manzi S J, Torrez Herrera J J and Pereyra V D 2012 Single-file diffusion in a box: effect of the initial configuration *Phys. Rev.* E **86** 021129
[13] Kutner R 1981 Chemical diffusion in the lattice gas of non-interacting particles *Phys. Lett.* A **81** 239–40
[14] Chou T, Mallick K and Zia R K P 2011 Non-equilibrium statistical mechanics: from a paradigmatic model to biological transport *Rep. Prog. Phys.* **74** 116601
[15] Akella J S, Wloga D, Kim J, Starostina N G, Lyons-Abbott S, Morrissette N S, Dougan S T, Kipreos E T and Gaertig J 2010 MEC-17 is an alpha-tubulin acetyltransferase *Nature* **467** 218–22
[16] Shida T, Cueva J G, Xu Z, Goodman M B and Nachury M V 2010 The major alpha-tubulin K40 acetyltransferase alphaTAT1 promotes rapid ciliogenesis and efficient mechanosensation *Proc. Natl Acad. Sci. USA* **107** 21517–22
[17] Montagnac G, Meas-Yedid V, Irondelle M, Castro-Castro A, Franco M, Shida T, Nachury M V, Benmerah A, Olivo-Marin J-C and Chavrier P 2013 αTAT1 catalyses microtubule acetylation at clathrin-coated pits *Nature* **502** 567–70
[18] Szyk A, Deaconescu A M, Spector J, Goodman B, Valenstein M L, Ziolkowska N E, Kormendi V, Grigorieff N and Roll-Mecak A 2014 Molecular basis for age-dependent microtubule acetylation by tubulin acetyltransferase *Cell* **157** 1405–15
[19] Rödenbeck C, Kärger J and Hahn K 1998 Calculating exact propagators in single-file systems via the reflection principle *Phys. Rev.* E **57** 4382–97
[20] Odde D 1998 Diffusion inside microtubules *Eur. Biophys. J.* **27** 514–20
[21] Crank J 1975 *The Mathematics of Diffusion* (Oxford: Oxford University Press)
[22] Gumbel E J 1958 *Statistics of Extremes* (New York: Columbia University Press)
[23] Stern A S and Berg H C 2013 Single-file diffusion of flagellin in flagellar filaments *Biophys. J.* **105** 182–4
[24] Yang S Y, Yang J-A, Kim E-S, Jeon G, Oh E J, Choi K Y, Hahn S K and Kim J K 2010 Single-file diffusion of protein drugs through cylindrical nanochannels *ACS Nano* **4** 3817–22
[25] Berg H C and Purcell E M 1977 Physics of chemoreception *Biophys. J.* **20** 193
[26] Milo R 2013 What is the total number of protein molecules per cell volume? A call to rethink some published values *Bioessays* **35** 1050–5
[27] Wang M, Herrmann C J, Simonovic M, Szklarczyk D and von Mering C 2015 Version 4.0 of PaxDb: Protein abundance data, integrated across model organisms, tissues, and cell-lines *Proteomics* **15** 3163–8
[28] Garvalov B K *et al* 2006 Luminal particles within cellular microtubules *J. Cell. Biol.* **174** 759–65
[29] Meyvis T K L, de Smedt S C, van Oostveldt P and Demeester J 1999 Fluorescence recovery after photobleaching: a versatile tool for mobility and interaction measurements in pharmaceutical research *Pharm. Res.* **16** 1153–62